

# Efficient Removal of Florasulam Herbicide from Water by Carboxymethyl Cellulose-Magnetic Graphene Oxide Nanocomposites

Mostafa A. I. Taha<sup>1\*</sup>, Mohamed E. I. Badawy<sup>1</sup>, Reda K. Abdel-Razik<sup>2</sup>, Mahmoud M. Abo-El-Saad<sup>1</sup>

## ABSTRACT

In this work, carboxymethyl cellulose-magnetic graphene oxide nanoparticles (CMC-MGO-NPs) were prepared for the removal of florasulam herbicide from aqueous media. The nanoparticles were characterized using Scanning Electron Microscopy (SEM), Dynamic Light Scattering (DLS), and Fourier Transform Infrared Spectroscopy (FTIR). Firstly, graphene oxide (GO) was obtained from graphite and then combined with Fe<sub>3</sub>O<sub>4</sub> to form magnetic graphene oxide nanoparticles (MGO-NPs). Secondly, MGO-NPs reacted with carboxymethyl cellulose (CMC) in the presence of calcium chloride (CaCl<sub>2</sub>) as a crosslinking agent producing CMC-MGO-NPs. Throughout the optimization of the removal process, several significant factors including pesticide concentration, adsorbent amount, temperature, pH, agitation time, and ionic strength were studied in detail using the Plackett–Burman design. The results showed that the maximum removal efficiency of florasulam reached 93.82% at an adsorbent amount of 75 mg, pH 5, agitation time of 30 min, and 40°C. In addition, the adsorption capacity and enrichment factor were 1.15 mg/g and 0.06 ug/mL, respectively. Considering the high removal efficiency, adsorption capacity, and enrichment factor, CMC-MGO-NPs could be promising adsorbents for removing pesticide residues from wastewater.

**Keywords:** Carboxymethyl Cellulose-Magnetic Graphene Oxide Nanoparticles; Florasulam; Removal; HPLC Analysis.

## INTRODUCTION

Herbicides are widely used in agriculture and play a vital role in ensuring good crop yields and harvests (Kniss 2017). According to global statistics, pesticide consumption rates amounted to \$52 billion in 2014, and this figure has now risen to \$62 billion and is expected to reach \$95 billion in 2025 (Khan et al. 2023). However, it is increasingly recognized that the widespread and non-standard use of pesticides harms the ecological environment (Faust et al. 1993). In practice, herbicides can enter water through spray drift, soil leaching, rainfall erosion, and surface runoff (Gustavsson et al. 2017). Additionally, some herbicides are persistent and can be detected year-round, leading to the prolonged exposure of freshwater and marine life to these potentially harmful chemicals (Marzonie et al. 2021). It has been reported that herbicide contamination of surface water has direct toxic effects on phytoplankton, epiphyte, and macrophyte populations (Cuppen et al. 1997). Moreover, some herbicides have been found to exert teratogenic, mutagenic, and endocrine-disrupting effects on aquatic organisms (McLachlan 2016).

Florasulam is a triazolopyrimidine sulfonanilide herbicide used for the post-emergence control of broadleaf weeds. Florasulam works by inhibiting acetolactate synthase (ALS) and is widely used for weed control in wheat crops and grasslands (Baghestani et al. 2007). Florasulam is polar and fairly water-soluble (its solubility in water is 6.36 g/L at 20°C, pH 7.0), and is also highly phytotoxic, thereby posing an environmental risk to crops, aquatic plants, and microorganisms (Jabusch and Tjeerdema 2008). Florasulam has been detected in rivers in the Midwestern United States (Furlong et al. 2000).

For living beings, water is one of the most indispensable elements because global health and development rely on it (Catley-Carlson 2019). However, water quality is gradually decreasing because of its contamination with a wide range of harmful substances such as agrochemicals, dyes, pharmaceuticals, and personal care products. Therefore, the search for new technologies to ensure the supply of water and reduce its pollution is mandatory (Gehrke et al. 2015). In the present context, nanoparticles are fast emerging as potent candidates for water treatment by adsorption mechanisms (Dinesha et al. 2017). Adsorption is a simple and effective tool for agricultural wastewater

---

DOI: 10.21608/esm.2024.363683

<sup>1</sup>Department of Pesticide Chemistry and Technology, Faculty of Agriculture, 21545-El-Shatby, Alexandria University, Alexandria, Egypt.

<sup>2</sup>Mammalian Toxicology Department, Central Agricultural Pesticide Laboratory, Agricultural Research Center, 21616-El-Sabahia, Alexandria, Egypt.

\* Correspondence to Mostafa A. I. Taha, Department of Pesticide Chemistry and Technology, Faculty of Agriculture, Aflatoun St., 21545-El-Shatby, Alexandria University; Alexandria, Egypt. Phone: 002039575269; Fax: 002035972780; E-mail: mostafa.taha@alexu.edu.eg

Received, May 25, 2024, Accepted, June 30, 2024.

treatment due to its widespread adaptability, environment-friendly, and low cost (Ghasemi et al. 2017). In addition, this method has the flexibility to regenerate and recycle the adsorbent, and the formation of secondary pollutants is rare (Dolatabadi et al. 2022). Among the nanoparticles, the combination of magnetic graphene oxide nanoparticles (MGO-NPs) and carboxymethyl cellulose (CMC) produced carboxymethyl cellulose-magnetic graphene oxide nanoparticles (CMC-MGO-NPs) would result in higher adsorption capacity and enhance the functional properties (Dolatabadi et al. 2022). The surface of CMC-MGO-NPs is rougher compared to MGO-NPs, which show a higher surface area (Sirajudheen et al. 2020). CMC-MGO-NPs composite was used as an adsorbent for removing chlorpyrifos from groundwater (Dolatabadi et al. 2022). In a similar investigation, CMC-MGO-NPs were used for the removal of atrazine from an aqueous phase (Khawaja et al. 2021).

In the current work, a simple approach was developed to prepare the CMC-MGO-NPs composite via a chemical deposition method. The chemical and physical characteristics of the prepared composites were evaluated using Scanning Electron Microscopy (SEM), Dynamic Light Scattering (DLS), and Fourier Transform Infrared Spectroscopy (FTIR). The main parameters, including pesticide concentration, adsorbent amount, temperature, pH, agitation time, and ionic strength were investigated to determine the removal efficiency.

## MATERIALS AND METHODS

### Chemicals

Technical grade of florasulam (96%) was supplied from Shoura Chemicals Co. (Giza, Cairo- Alexandria Desert Road, Egypt) (Figure 1). Graphite powder and carboxymethyl cellulose (CMC) were purchased from Sigma-Aldrich Chemical Co. (St. Louis, MO, USA).

Acetonitrile, methanol, and water of HPLC grade (99%) were purchased from Merck (Darmstadt, Germany). Polyvinylidene fluoride (PVDF) syringe filter (0.2  $\mu\text{m}$ ) (Puradisc, Whatman, USA). Other commercially available solvents and chemicals were of analytical grade and purchased from El-Gomhouria for Trading Chemicals and Medical Appliances Co., (Adeb Ishak St, Manshia, Alexandria, Egypt) and used without further purification.

### Preparation of carboxymethyl cellulose-magnetic graphene oxide nanoparticles (CMC-MGO-NPs)

Magnetic graphene oxide nanoparticles (MGO-NPs) were firstly prepared by combining graphene oxide (GO), derived from graphite, with  $\text{Fe}_3\text{O}_4$ . Then, a co-precipitation method was used to prepare CMC-MGO-NPs. This involved reacting the MGO-NPs with carboxymethylcellulose (CMC) as (1:3, w/w) ratio in the presence of calcium chloride ( $\text{CaCl}_2$ ), which acted as a crosslinking agent (Dolatabadi et al. 2022; Sirajudheen et al. 2020) as illustrated in Figure 2. A suspension containing MGO-NPs (1 g) in 50 mL of distilled water was prepared and sonicated for 15 min under a sonication power (75 kHz and pulses 9 cycles/sec). The sonicated mixture was vigorously mixed for 3 h using a magnetic stirrer. The aqueous solution containing CMC (3 g) in 100 mL of distilled water was prepared and blended with MGO-NPs solution and stirred at 70°C to prepare CMC-MGO-NPs. The CMC-MGO-NPs composite was formed and stabilized by adding drops of 0.1 M  $\text{CaCl}_2$  and left undisturbed for 12 h. This assists in the formation of a robust composite matrix that can be separated using a magnet. The precipitated composite was obtained using a magnet, and washed with ethanol followed with distilled water. The resulting CMC-MGO-NPs composite was placed in an oven at 80°C for 60 h to remove moisture.

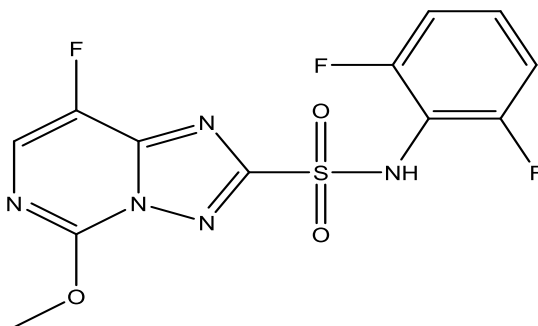
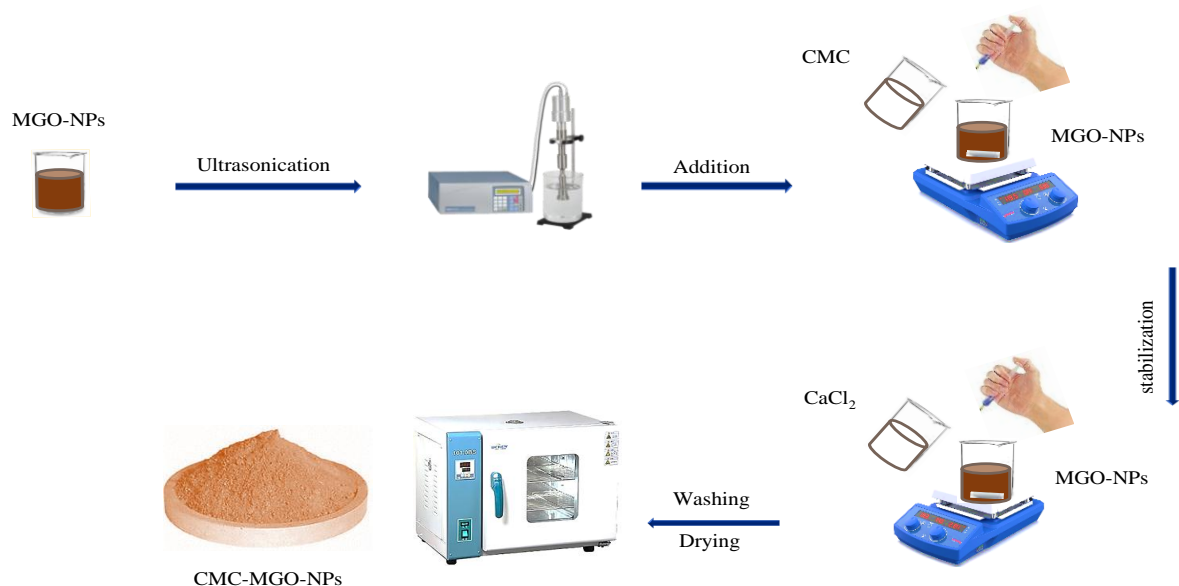


Fig. 1. Chemical structure of Florasulam



**Fig.2. Schematized diagram of CMC-MGO-NPs preparation**

### Characterizations of CMC-MGO-NPs

The morphology of the nanoparticles was examined using a JEOL-JSM5300 scanning electron microscope (SEM) located at the Faculty of Science, Alexandria University, Egypt. The size and distribution of the nanoparticles, characterized by particle size (nm) and polydispersity index (PDI), were measured using a Dynamic Light Scattering (DLS) at room temperature. The size of the particle was reported as the average diameter in nanometers (Mibielli et al. 2021; Silva et al. 2012). Fourier Transform Infrared Spectroscopy (FTIR, Perkin Elmer) was used to identify the functional groups present on the nanoparticles (Badawy et al. 2016).

### Removal of florasulam by CMC-MGO-NPs

A design of experiments (DOE) approach was used to optimize this material's performance. This involved studying how various factors (pesticide concentration, adsorbent amount, temperature, pH, agitation time, and ionic strength) affected the removal of florasulam. A full factorial design (13 runs including the center point) was implemented using MINITAB™ software v17.1.0 (Minitab Inc., State College, PA, USA), with each factor investigated at three levels (low, medium, and high), coded as -1, 0, and +1, respectively (Table 1).

**Table 1. Experimental design using Minitab software for removal of florasulam**

Run order	Pesticide concentration (µg/mL)	Adsorbent Amount (mg)	Temperature (°C)	pH	Agitation Time (min)	Ionic strength (%)
1	+1 (75)	-1 (25)	+1 (40)	-1 (5)	-1 (10)	-1 (0)
2	+1 (75)	+1 (75)	-1 (10)	+1 (9)	-1 (10)	-1 (0)
3	-1 (25)	+1 (75)	+1 (40)	-1 (5)	+1 (30)	-1 (0)
4	+1 (75)	-1 (25)	+1 (40)	+1 (9)	-1 (10)	+1 (10)
5	+1 (75)	+1 (75)	-1 (10)	+1 (9)	+1 (30)	-1 (0)
6	+1 (75)	+1 (75)	+1 (40)	-1 (5)	+1 (30)	+1 (10)
7	-1 (25)	+1 (75)	+1 (40)	+1 (9)	-1 (10)	+1 (10)
8	-1 (25)	-1 (25)	+1 (40)	+1 (9)	+1 (30)	-1 (0)
9	-1 (25)	-1 (25)	-1 (10)	+1 (9)	+1 (30)	+1 (10)
10	+1 (75)	-1 (25)	-1 (10)	-1 (5)	+1 (30)	+1 (10)
11	-1 (25)	+1 (75)	-1 (10)	-1 (5)	-1 (10)	+1 (10)
12	-1 (25)	-1 (25)	-1 (10)	-1 (5)	-1 (10)	-1 (0)
13	0 (50)	0 (50)	0 (25)	0 (7)	0 (20)	0 (5)

-1: Lowest value, +1: Highest value and 0: Center point.

Finally, a statistical analysis was conducted to identify which factors significantly affect pesticide removal. This analysis will involve a polynomial equation ( $Y = A_0 + A_1X_1 + A_2X_2 + A_3X_3 + A_nX_n$ ) that expresses the dependent variable (Y, removal %) as a function of independent factors ( $X_1$  to  $X_n$ ). In this equation,  $A_0$  represents a constant value, while  $A_1$  to  $A_n$  are the coefficients associated with each independent factor (Mathews 2004).

Aqueous solutions containing varying concentrations (25, 50, and 75  $\mu\text{g/mL}$ ) of florasulam and added to Eppendorf tubes containing nanoparticles, with a total volume of 2 mL. The experiment was conducted under different conditions to assess effectiveness. After that, a magnet separated the nanoparticles from the solution. The remaining liquid was filtered through a syringe filter 0.22  $\mu\text{m}$  and then analyzed by HPLC to determine the residues of florasulam (Hou et al. 2021; Shrivastava et al. 2017). The HPLC conditions were mobile phase of acetonitrile and methanol (70:30) at a flow rate of 1.3 mL/min, 210 nm optimal wavelength with a ZORBAX Eclips Plus C18 column (250 $\times$ 4.6 mm id, 5  $\mu\text{m}$  particle size). The following equations were used to calculate the percentage of removal (Equation 1), the adsorption capacity ( $q_e$ , Equation 2), and the enrichment factor (EF, Equation 3).

$$\text{Removal (\%)} = \frac{(C_i - C_e)}{C_i} \times 100 \quad \dots\dots(1)$$

$$q_e = \frac{(C_i - C_e)}{m} \times V \quad \dots\dots(2)$$

$$\text{EF} = \frac{C_e}{C_i} \quad \dots\dots(3)$$

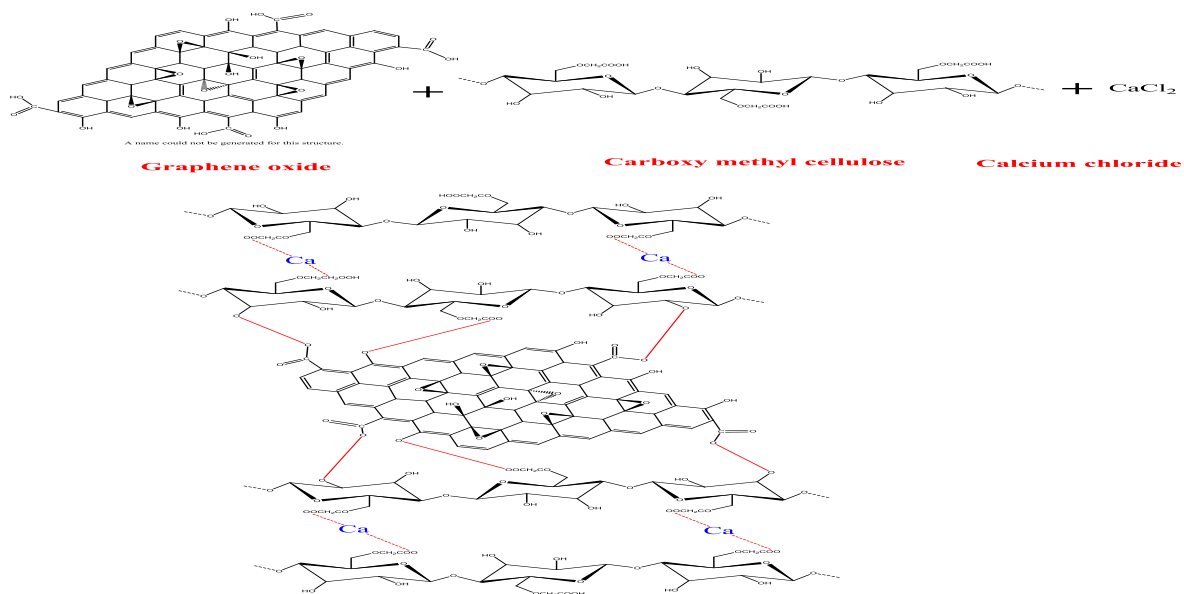


Fig.3. Proposed structure of CMC-MGO-NPs

Where,  $C_i$  is the initial concentration of the pesticide in the solution ( $\mu\text{g/mL}$ ),  $C_e$  is the equilibrium concentration of pesticide in the solution ( $\mu\text{g/mL}$ ),  $m$  is the mass of the adsorbent (g), and  $V$  is the volume of the solution (L).

### Statistical analysis

Data were presented as mean  $\pm$  standard error (SE). The statistical significance standard was set at  $p \leq 0.05$ . For data analysis, one-way variance analysis (ANOVA) was employed, followed by the Student-Newman-Keuls Test using IBM SPSS software version 25.0 (Statistical Package for Social Sciences, Chicago, IL, USA) (IBM 2017).

## RESULTS AND DISCUSSION

### Preparation and Characterizations of CMC-MGO-NPs

The product yield of CMC-MGO-NPs was 1.3 g with a light brown color. The proposed structures of CMC-MGO-NPs are presented in Figure 3. In short, GO can interact with CMC chains through physical bonds like hydrogen bonding and van der Waals forces. These bonds form between the carboxylic groups on CMC and the hydroxyl groups on GO sheets (Huang et al. 2017). Because of this good interaction and hydrogen bonding ability, GO can be easily dispersed through CMC microbeads, creating a network composite. Furthermore, the addition of calcium chloride ( $\text{CaCl}_2$ ) as a crosslinking agent improves the stability of the CMC-MGO-NPs composite. This creates a robust composite matrix that can be separated using magnets (Tuan Mohamood et al. 2021).



**Fig.4.** SEM of CMC-MGO-NPs. The images is spherical particles with scale bar 1  $\mu$  and magnification x 20000 and 20 KV

The surface morphology of CMC-MGO-NPs was examined using SEM. Figure 4 presents the obtained SEM images. As reported in the previous study (Dolatabadi et al. 2022), the images show a layered structure with uneven shapes, like a flat sheet with rounded edges. While SEM is a powerful technique for visualizing the shape and size (morphology) of nanoparticles, its limitations often necessitate the use of complementary methods for comprehensive material characterization.

The average particle size was found as 93.41 nm. PDI value was 0.331 which indicates a more uniform particle size distribution and stability at pH 7 and 25°C. According to the literature, a PDI between 0.05 and 0.7 indicates a good dispersed sample (Tang et al. 2012; Tyagi et al. 2012). FTIR is a very versatile tool for surface characterization of nanoparticles (Baraton and Merhari 2007). Figures 5A-5B show the FTIR spectra of CMC and CMC-MGO-NPs. Figure 5A shows the spectrum of CMC. The absorption peak at 3362  $\text{cm}^{-1}$  represents the OH groups. The -CH stretching vibration appeared at 2925  $\text{cm}^{-1}$ . Strong absorption peaks at 1617  $\text{cm}^{-1}$  and 1426  $\text{cm}^{-1}$  indicated the appearance of the asymmetrical and symmetrical stretching of the -COO- group. A significant stretching C-O vibration of primary alcohols and ethers in the cellulose backbone of the cellulose chain was observed at 1062  $\text{cm}^{-1}$ . The appearance of a peak at 1062  $\text{cm}^{-1}$  might be attributed to the C-O-C pyranose ring stretching vibration (Ibrahim et al. 2011).

In the FTIR spectra of the CMC-MGO-NPs composite (Figure 5B), a broad band at 3442  $\text{cm}^{-1}$  is attributed to the hydrogen bonds, and the stretching of O-H groups. The stretching of C-H bonds of glucose units in cellulose structure is shown by the characteristic peak at 2927  $\text{cm}^{-1}$ . The asymmetrical and symmetrical stretching vibrations of carboxylate groups are characterized by peaks at 1462 and 1633  $\text{cm}^{-1}$ . The stretching of the -C-O- bonds on the polysaccharide is shown by the peaks at 1024-1119  $\text{cm}^{-1}$  (Dolatabadi et al. 2022; Fulazzaky et al. 2017). The peak at 620  $\text{cm}^{-1}$  can

be attributed to the characteristic stretching of Fe-O bonds. When CMC is linked with MGO, the peaks at 3442  $\text{cm}^{-1}$  as a result of O-H stretching vibration, 1633  $\text{cm}^{-1}$  owing to COO- group presence, 1427  $\text{cm}^{-1}$  is for -CH<sub>2</sub> vibration originated from scissoring, implying GO interacted with CMC via hydrogen bonds and indicating both solutions were properly amalgamated (Shakil et al. 2024).

#### Florasulam removal by using CMC-MGO-NPs

The data for the removal of tested pesticides by CMC-MGO-NPs at different parameters are shown in Table 2. For florasulam, a wide range of removal efficiencies varies from 82.18% to 93.82%. Runs 2, 3, 5, and 7 had the highest removal with values of 92.58, 93.82, 91.56, and 90.18%, respectively. The runs 6, 11, and 13 were moderately (89.31, 86.18, and 88.77%, respectively). However, runs 1, 4, 8, 9, 10, and 12 had the lowest efficiency with values of 83.91, 85.15, 85.09, 85.45, 84.14, and 82.18 %, respectively. The adsorption capacity of CMC-MGO-NPs for florasulam presented that runs 1, 4, and 10 were the highest (9.95, 10.09, and 9.97 mg/g, respectively). The runs 2, 5, 6, 8, 9, 12, and 13 were moderate with (3.66, 3.62, 3.53, 3.12, 3.13, 3.01, and 3.43mg/g, respectively). Nevertheless, runs 3, 7, and 11 exhibited low adsorption capacity (1.15, 1.10, and 1.05 mg/g, respectively). EF is a key metric used in pesticide residue analysis and refers to the fold increase in the concentration of a pesticide after the adsorption and extraction processes. It indicates how much more concentrated the pesticide is in the final extract compared to its initial concentration in the sample. A high EF allows for the detection of very low levels of pesticides. Moreover, the data of EF of CMC-MGO-NPs for florasulam are presented in Table 2. Experiments 1, 4, 8, 9, 10, and 12 proved the highest values of 0.16, 0.15, 0.15, 0.15, 0.16, and 0.18  $\mu\text{g/mL}$ , respectively. Runs 6, 11, and 13 were moderate in EF (0.11, 0.14, and 0.11, respectively). However, experiments 2, 3, 5, and 7 were the lowest (0.07, 0.06, 0.08, and 0.10, respectively).

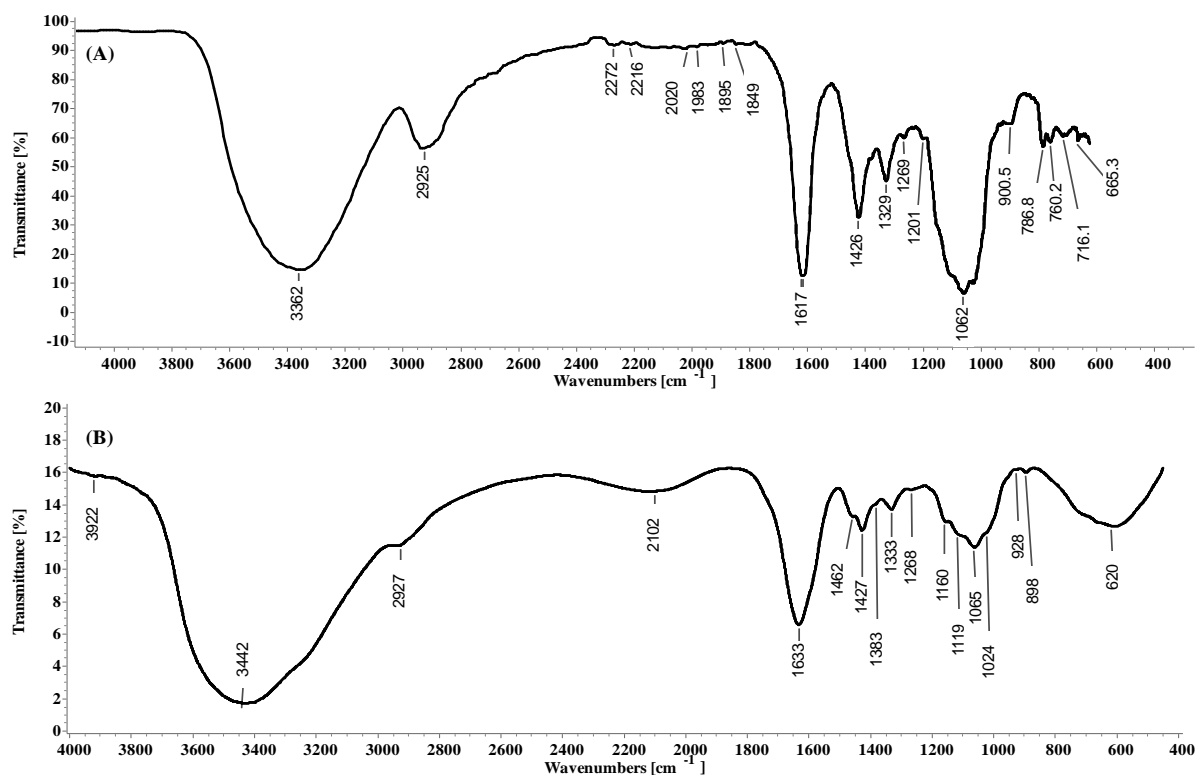
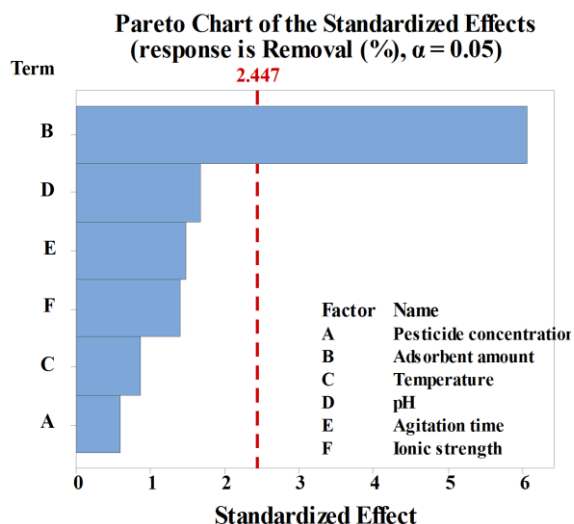


Fig. 5. FTIR spectra of CMC (A) and CMC-MGO-NPs (B)

Table 2. Efficiency of CMC-MGO-NPs in removal of florasulam

Run	Added amount ( $\mu\text{g}$ ) $\pm$ SE	Found amount ( $\mu\text{g}$ ) $\pm$ SE	Adsorbed amount ( $\mu\text{g}$ ) $\pm$ SE	Non-extracted amount ( $\mu\text{g}$ ) $\pm$ SE	Removal (%) $\pm$ SE	Adsorption capacity (mg/g) $\pm$ SE	Enrichment factor ( $\mu\text{g/mL}$ ) $\pm$ SE
1	150	23.83 $\pm$ 1.35	123.00 $\pm$ 0.77	3.17 $\pm$ 0.58	83.91 <sup>d</sup> $\pm$ 0.91	9.95 <sup>a</sup> $\pm$ 0.11	0.16 <sup>a</sup> $\pm$ 0.009
2	150	11.00 $\pm$ 1.06	136.33 $\pm$ 0.39	2.67 $\pm$ 0.67	92.58 <sup>ab</sup> $\pm$ 0.72	3.66 <sup>b</sup> $\pm$ 0.03	0.07 <sup>cd</sup> $\pm$ 0.007
3	50	2.83 $\pm$ 0.39	46.67 $\pm$ 0.58	0.50 $\pm$ 0.19	93.82 <sup>a</sup> $\pm$ 0.84	1.15 <sup>e</sup> $\pm$ 0.01	0.06 <sup>d</sup> $\pm$ 0.008
4	150	22.00 $\pm$ 0.48	126.00 $\pm$ 0.96	2.00 $\pm$ 1.45	85.15 <sup>cd</sup> $\pm$ 0.33	10.09 <sup>a</sup> $\pm$ 0.04	0.15 <sup>ab</sup> $\pm$ 0.003
5	150	12.50 $\pm$ 0.96	134.67 $\pm$ 0.96	2.83 $\pm$ 1.93	91.56 <sup>ab</sup> $\pm$ 0.65	3.62 <sup>b</sup> $\pm$ 0.03	0.08 <sup>cd</sup> $\pm$ 0.007
6	150	15.83 $\pm$ 1.54	132.00 $\pm$ 0.58	2.17 $\pm$ 0.96	89.31 <sup>bc</sup> $\pm$ 1.04	3.53 <sup>bc</sup> $\pm$ 0.04	0.11 <sup>bc</sup> $\pm$ 0.010
7	50	4.50 $\pm$ 0.58	43.67 $\pm$ 0.39	1.83 $\pm$ 0.19	90.18 <sup>ab</sup> $\pm$ 1.26	1.10 <sup>e</sup> $\pm$ 0.02	0.10 <sup>cd</sup> $\pm$ 0.013
8	50	6.83 $\pm$ 0.77	42.33 $\pm$ 0.39	0.83 $\pm$ 0.39	85.09 <sup>cd</sup> $\pm$ 1.68	3.12 <sup>d</sup> $\pm$ 0.06	0.15 <sup>ab</sup> $\pm$ 0.017
9	50	6.67 $\pm$ 0.67	41.33 $\pm$ 0.58	2.00 $\pm$ 0.10	85.45 <sup>cd</sup> $\pm$ 1.47	3.13 <sup>d</sup> $\pm$ 0.05	0.15 <sup>ab</sup> $\pm$ 0.015
10	150	23.50 $\pm$ 0.77	125.67 $\pm$ 1.16	0.83 $\pm$ 0.39	84.14 <sup>d</sup> $\pm$ 0.52	9.97 <sup>a</sup> $\pm$ 0.06	0.16 <sup>a</sup> $\pm$ 0.005
11	50	6.33 $\pm$ 0.29	42.67 $\pm$ 0.19	1.00 $\pm$ 0.10	86.18 <sup>cd</sup> $\pm$ 0.63	1.05 <sup>e</sup> $\pm$ 0.01	0.14 <sup>ab</sup> $\pm$ 0.006
12	50	8.17 $\pm$ 0.39	40.33 $\pm$ 0.77	1.50 $\pm$ 0.39	82.18 <sup>d</sup> $\pm$ 0.84	3.01 <sup>d</sup> $\pm$ 0.03	0.18 <sup>a</sup> $\pm$ 0.008
13	100	10.83 $\pm$ 0.96	87.00 $\pm$ 1.16	2.17 $\pm$ 0.19	88.77 <sup>bc</sup> $\pm$ 1.00	3.43 <sup>c</sup> $\pm$ 0.04	0.11 <sup>bc</sup> $\pm$ 0.010

Values are mean of three replicates and are given as mean  $\pm$  standard error. Different letters in the same column indicate significant differences according to Student–Newman–Keuls (SNK) test ( $P \leq 0.05$ ).



**Fig. 6. Pareto Chart of the standardized effects of pesticide concentration, adsorbent amount, temperature, pH, agitation time, and ionic strength on the adsorption of florasulam, on CMC-MGO-NPs (response is removal (%),  $\alpha = 0.05$ )**

To investigate the main effect of tested factors on the adsorptive removal of florasulam by CMC-MGO-NPs, a Pareto chart was performed, and the results are shown in Figure 6. The factor of the adsorbent amount had the most significant effect at  $\alpha = 0.05$ . Followed by pH, agitation time, ionic strength, temperature, and pesticide concentration. These factors were not significant because they showed values lower than the reference line (2.447 at  $\alpha = 0.05$ ). The model for removal prediction of florasulam is as follows (Equation 4).

$$\text{Removal (\%)} = 76.05 + 0.0125 \text{ Pesticide concentration} + 0.1257 \text{ Adsorbent amount} + 0.0299 \text{ Temperature} + 0.436 \text{ pH} + 0.0766 \text{ Agitation time} - 0.145 \text{ Ionic strength}$$

... (4)

$S = 1.80$  and  $R^2 = 88.18\%$

It can be seen that the ionic strength factor had a negative coefficient indicating a decrease in adsorption with the increase of this factor. However, other factors presented a positive coefficient.

Overall, CMC-MGO-NPs offer a promising approach to pesticide removal due to their high adsorption capacity, magnetic separation, and potential biocompatibility (Dolatabadi et al. 2022). Therefore, the CMC-MGO-NPs allow to adsorb high amounts of pesticide molecules onto their surface. Different studies have shown successful adsorption of different pesticides, including Atrazine and chlorpyrifos from an aqueous solution by CMC-MGO-NPs (Dolatabadi et al. 2022; Khawaja et al. 2021). In addition, adsorptive

removal of toxic azo dyes from water using CMC-MGO-NPs (Sirajudheen et al. 2020).

## CONCLUSION

In recent years, the adsorption of pollutants on nanoparticles has been gaining widespread attention, especially in the water treatment process. This study revealed the successful synthesis of low-cost, magnetic graphene oxide modified with carboxymethyl cellulose exhibiting excellent affinity towards pesticides due to anionic functional groups, surface roughness, and the porous structure confirmed by relevant spectrometric techniques. Optimizing the adsorption process by influencing parameters like pesticide concentration, adsorbent amount, temperature, pH, agitation time and ionic strength validated CMC-MGO-NPs suitability as good adsorbent. CMC-MGO-NPs have a massive potential to be used as environmentally friendly, highly effective, and good stability adsorbents. Therefore, CMC-MGO-NPs offer promising and excellent adsorbent material for the sustainable application of the material in the wastewater purification process. In addition, the kinetic and isotherm studies are still under investigation. However, we need further toxicological studies for risk assessment demonstration in wide applications.

## FUNDING

This research did not receive any grant or specific funding from funding agencies in the public, commercial, or not-for-profit sectors.

## REFERENCES

Badawy, M.E., E.I.Rabea., N.E. Taktak, M.A. El Nouby. 2016. Production and properties of different molecular weights of chitosan from marine shrimp shells. *J. of Chitin and Chitosan Sci.* 4(1):46-54.

Baghestani, M.A., E. Zand, S. Soufizadeh, N. Bagherani, R. Deihimfard. 2007. Weed control and wheat (*Triticum aestivum* L.) yield under application of 2, 4-D plus carfentrazone-ethyl and florasulam plus flumetsulam: Evaluation of the efficacy. *Crop Protection* 26(12):1759-1764.

Baraton, M.I. and L.Merhari. 2007. Dual contribution of FTIR spectroscopy to nanoparticles characterization: surface chemistry and electrical properties. In: *Nanomaterials synthesis, interfacing, and integrating in devices, circuits, and systems II.* vol 6768. SPIE, p 38-47.

Catley-Carlson, M. 2019. The water paradox: overcoming the global crisis in water management. *Nature* 565(7740):426-427.

Cuppen, J.G., P.J. Van den Brink, H.Van der Woude, N. Zwaardemaker and T.C. Brock. 1997. Sensitivity of macrophyte-dominated freshwater microcosms to chronic levels of the herbicide linuron. *Ecotoxicology and Environmental Safety* 38(1):25-35.

- Dinesha, B., H. Sharanagouda, N. Udaykumar, C. Ramachandr and A.B. Dandekar. 2017. Removal of pollutants from water/waste water using nano-adsorbents: a potential pollution mitigation. *Int J Curr Microbiol Appl Sci.* 6(10):4868-4872.
- Dolatabadi, M., H. Naidu and S. Ahmadzadeh. 2022. Adsorption characteristics in the removal of chlorpyrifos from groundwater using magnetic graphene oxide and carboxy methyl cellulose composite. *Separation and Purification Technology.* 300:121919
- Faust, M., R. Altenburger, W. Boedeker and L. Grimme. 1993. Additive effects of herbicide combinations on aquatic non-target organisms. *Sci. of the total environment.* 134:941-952.
- Fulazzaky, M.A., Z. Majidnia and A. Idris. 2017. Mass transfer kinetics of Cd (II) ions adsorption by titania polyvinylalcohol-alginate beads from aqueous solution. *Chemical Engineering J.* 308:700-709.
- Furlong, E.T., M.R. Burkhardt, P.M. Gates, S.L. Werner and W.A. Battaglin. 2000. Routine determination of sulfonyleurea, imidazolinone, and sulfonamide herbicides at nanogram-per-liter concentrations by solid-phase extraction and liquid chromatography/mass spectrometry. *Sci. of the Total Environment.* 248(2-3):135-146.
- Gehrke, I., A. Geiser and A. Somborn-Schulz. 2015. Innovations in nanotechnology for water treatment. *Nanotechnology, sci. and applications:*1-17.
- Ghasemi E, Heydari A, Sillanpää M (2017) Superparamagnetic Fe<sub>3</sub>O<sub>4</sub>@ EDTA nanoparticles as an efficient adsorbent for simultaneous removal of Ag (I), Hg (II), Mn (II), Zn (II), Pb (II) and Cd (II) from water and soil environmental samples. *Microchemical Journal* 131:51-56
- Gustavsson M, Kreuger J, Bundschuh M, Backhaus T (2017) Pesticide mixtures in the Swedish streams: environmental risks, contributions of individual compounds and consequences of single-substance oriented risk mitigation. *Science of the total environment* 598:973-983
- Hou X, Ding R, Yan S, Zhao H, Yang Q, Wu W (2021) ZrO<sub>2</sub> nanoparticles and poly (diallyldimethylammonium chloride)-doped graphene oxide aerogel-coated stainless-steel mesh for the effective adsorption of organophosphorus pesticides. *Foods* 10(7):1616
- IBM (2017) Corp. Released 2017. IBM SPSS Statistics for Windows, Version 25.0. . Armonk, NY: IBM Corp
- Ibrahim AA, Adel AM, Abd El-Wahab ZH, Al-Shemy MT (2011) Utilization of carboxymethyl cellulose based on bean hulls as chelating agent. Synthesis, characterization and biological activity. *Carbohydrate polymers* 83(1):94-115
- Jabusch TW, Tjeerdema RS (2008) Chemistry and fate of triazolopyrimidine sulfonamide herbicides. *Reviews of environmental contamination and toxicology:*31-52
- Khan BA, et al. (2023) Pesticides: impacts on agriculture productivity, environment, and management strategies Emerging contaminants and plants: Interactions, adaptations and remediation technologies. Springer, p 109-134
- Khawaja H, Zahir E, Asghar MA, Rafique K, Asghar MA (2021) Synthesis and application of covalently grafted magnetic graphene oxide carboxymethyl cellulose nanocomposite for the removal of atrazine from an aqueous phase. *Journal of Macromolecular Science, Part B* 60(12):1025-1044
- Kniss AR (2017) Long-term trends in the intensity and relative toxicity of herbicide use. *Nature communications* 8(1):1-7
- Marzoni M, et al. (2021) Toxicity thresholds of nine herbicides to coral symbionts (Symbiodiniaceae). *Scientific Reports* 11(1):21636
- Mathews PG (2004) Design of Experiments with MINITAB. Quality press
- McLachlan JA (2016) Environmental signaling: from environmental estrogens to endocrine-disrupting chemicals and beyond. *Andrology* 4(4):684-694
- Mibielli RBI, Gerber T, Mazzarino L, Veleirinho MB, Yunes RA, Maraschin M (2021) Development of a spectrophotometric method for quantification of carvacrol in nanoemulsions. *Revista Brasileira de Farmacognosia* 31(1):116-120 doi:<https://doi.org/10.1007/s43450-021-00134-9>
- Mojiri A, et al. (2020) Pesticides in aquatic environments and their removal by adsorption methods. *Chemosphere* 253:126646
- Shakil MSR, Aktar MS, Hossain MA, Ahmed S (2024) Synthesis and application of carboxymethyl cellulose-graphene oxide composite for the mitigation of Pb<sup>2+</sup> and Cd<sup>2+</sup> from aqueous solution. *Cleaner Engineering and Technology* 18:100724
- Shrivastava K, Ghosale A, Nirmalkar N, Srivastava A, Singh SK, Shinde SS (2017) Removal of endrin and dieldrin isomeric pesticides through stereoselective adsorption behavior on the graphene oxide-magnetic nanoparticles. *Environmental Science and Pollution Research* 24:24980-24988
- Silva AL, et al. (2012) Physical factors affecting plasmid DNA compaction in stearylamine-containing nanoemulsions intended for gene delivery. *Pharmaceuticals* 5(6):643-654 doi:<https://doi.org/10.3390/ph5060643>
- Sirajudheen P, Nikitha MR, Karthikeyan P, Meenakshi S (2020) Perceptive removal of toxic azo dyes from water using magnetic Fe<sub>3</sub>O<sub>4</sub> reinforced graphene oxide-carboxymethyl cellulose recyclable composite: Adsorption investigation of parametric studies and their mechanisms. *Surfaces and Interfaces* 21:100648
- Tang SY, Manickam S, Wei TK, Nashiru B (2012) Formulation development and optimization of a novel Cremophore EL-based nanoemulsion using ultrasound cavitation. *Ultrasonics Sonochemistry* 19(2):330-345 doi:<https://doi.org/10.1016/j.cocis.2005.06.004>
- Tyagi S, Panda A, Khan S (2012) Formulation and evaluation of diclofenac diethyl amine microemulsion incorporated in hydrogel. *World Journal of Pharmaceutical Research* 1:1298-319.

## الملخص العربي

### كفاءة إزالة مبيد الحشائش فلوراسولام من الماء بواسطة مركبات كربوكسي ميثيل سليولوز - أكسيد الجرافين المغناطيسي النانوية

مصطفى أحمد إبراهيم طه<sup>١</sup>، محمد الطاهر إبراهيم بدوي<sup>١</sup>، رضا خميس عبدالرازق<sup>٢</sup>، محمود مسعود أبوالسعد<sup>١</sup>

(CMC-MGO). خلال تجارب الإزالة المختلفة، تمت دراسة العديد من العوامل المهمة بما في ذلك تركيز المبيد وكمية المادة المادصة ودرجة الحرارة والرقم الهيدروجيني ووقت الإمتزاز والقوة الأيونية باستخدام تصميم بلاكيت بيرمان. أظهرت النتائج أن أقصى كفاءة لإزالة الفلوراسولام وصلت إلى ٩٣,٨٢٪ عند كمية مادة مادصة ٧٥ مجم ودرجة حموضة ٥ ووقت إمتزاز ٣٠ دقيقة و ٤٠ درجة مئوية. بالإضافة إلى ذلك، كانت سعة الإدمصاص وعامل الإثراء ١,١٥ مجم/جم و ٠,٠٦ ميكروجرام/مل على التوالي. بالنظر إلى كفاءة الإزالة العالية وسعة الإدمصاص وعامل الإثراء، يمكن أن تكون مركبات كربوكسي ميثيل سليولوز - أكسيد الجرافين المغناطيسي النانوية مواد مادصة واعدة لإزالة بقايا المبيدات من المياه الملوثة.

في هذا البحث، تم تحضير جسيمات نانوية من كربوكسي ميثيل سليولوز - أكسيد الجرافين المغناطيسي (CMC-MGO-NPs) لإزالة مبيد الحشائش فلوراسولام من الوسط المائي. وقد تم توصيف الجسيمات النانوية المحضرة باستخدام المجهر الإلكتروني الماسح (SEM) والتشتت الضوئي الديناميكي (DLS) ومطياف الأشعة تحت الحمراء (FTIR). أولاً، تم الحصول على أكسيد الجرافين (GO) من الجرافيت ثم تم دمجه مع  $Fe_3O_4$  لتكوين جسيمات نانوية من أكسيد الجرافين المغناطيسي (MGO-NPs). ثانياً، تم تفاعل جسيمات أكسيد الجرافين المغناطيسية مع كربوكسي ميثيل سليولوز (CMC) في وجود كلوريد الكالسيوم ( $CaCl_2$ ) كعامل ربط لإنتاج جسيمات من كربوكسي ميثيل سليولوز-أكسيد الجرافين المغناطيسية